scientific reports

Check for updates

OPEN

The CoREST complex is a therapeutic vulnerability in malignant peripheral nerve sheath tumors

Imad Soukar[1], Robert J. Fisher[1], Sanjana Bhagavatula[1], Marianne Collard[1], Philip A. Cole[2] & Rhoda M. Alani[1]✉

Malignant peripheral nerve sheath tumor (MPNST) is a highly aggressive sarcoma that may be seen in patients with neurofibromatosis type 1 (NF1) or occur sporadically. While surgery is the primary treatment for localized MPNST with a 61.9% overall survival rate, metastatic disease is often fatal due to resistance to systemic therapies which underscores the urgent need for effective treatments. MPNSTs frequently harbor inactivating driver mutations in the PRC2 epigenetic repressor complex suggesting epigenetic therapies may represent a specific vulnerability in these tumors. Here, we investigate the role of the LSD1-HDAC1-CoREST (LHC) repressor complex in mediating MPNST tumor growth and progression. Our findings demonstrate that the LHC small molecule inhibitor, corin, induces apoptosis and significantly inhibits proliferation in MPNST cells. Transcriptomic analysis of corin-treated MPNST cells demonstrates specific increases in genes associated with axonogenesis and neuronal differentiation as well as altered extracellular matrix; additionally, corin treatment is shown to inhibit MPNST invasion in vitro. These results underscore the critical role of the LHC complex in facilitating MPNST growth and progression and suggest that targeting the LHC complex represents a promising therapeutic approach for this aggressive malignancy.

Keywords CoREST, Corin, HDAC, LSD1, MPNST, Epigenetics

Malignant peripheral nerve sheath tumors (MPNSTs) are rare soft tissue sarcomas which are typically treated by surgical resection with a relatively high recurrence rate[1], and are frequently prone to metastasis[2]. Patients with a germline mutation in the tumor suppressor gene, neurofibromatosis type 1 (NF1), carry a lifetime susceptibility to MPNST and account for over 50% of cases, with roughly 10% of NF1 patients developing MPNST[3], while sporadic MPNSTs may also carry NF1 mutations and occur at a rate of 0.001%[4–6]. MPNSTs frequently possess inactivating mutations in genes associated with polycomb repressor complex 2 (PRC2)[7,8] suggesting that epigenetic approaches to therapy may prove successful. Despite convincing evidence that epigenetic therapies including BET bromodomain inhibitors[9] and HDAC inhibitors[10,11] may prove useful in patients with MPNST, clinical studies have not demonstrated successful responses to date largely due to the narrow therapeutic window of such drugs in solid tumors[12,13] as well as acquired resistance mechanisms to such therapies[14–17].

Our laboratory recently discovered a potent and selective inhibitor of the LHC repressor complex, corin, which has proven effective at inhibiting tumor cell growth in melanoma, cutaneous squamous cell carcinoma, diffuse intrinsic pontine glioma (DIPG) and breast cancers[18–20]. The bifunctional nature of this inhibitor allows for targeting of both the histone deacetylase (HDAC) and lysine-specific demethylase 1 (LSD1) functions of the LHC complex and has demonstrated increased potency and an improved therapeutic window versus the corresponding Class I HDAC inhibitor (entinostat) or LSD1 inhibitor (GSK-LSD1) alone[18,21]. Additionally, corin has proven effective in inhibiting tumor cell plasticity and reversing therapy resistance in human melanoma cells[21]. MPNST and melanoma tumor cells are both derived from the same embryonic neural crest cell lineage[22] and recent studies have determined that PRC2 loss in MPNST confers a dedifferentiated early neural crest phenotype[23] similar to that seen during melanoma phenotype switching[24]. As we have determined that the LHC inhibitor, corin, is able to block tumor cell growth, reverse phenotype switching and prevent establishment of

[1]Department of Dermatology, Boston University Chobanian and Avedisian School of Medicine, 609 Albany Street, J-507, Boston, MA 02118, USA. [2]Division of Genetics, Departments of Medicine and Biological Chemistry and Molecular Pharmacology, Harvard Medical School and Brigham and Women's Hospital, Boston, MA, USA. ✉email: alani@bu.edu

neural crest-associated lineages in melanoma[21], we hypothesized that inhibition of the LHC complex in MPNST would similarly block tumor cell growth and migration, with a preference for PRC2-negative tumors. Here, we show that corin treatment of MPNST cells leads to inhibition of tumor cell growth and increased apoptosis with a notably lower IC50 versus the HDAC inhibitor (HDACi) entinostat or the LSD1 inhibitor (LSD1i) GSK-LSD1. Interestingly, transcriptomic analysis demonstrates a specific role for the LHC complex in regulating expression of genes associated with MPNST neuronal differentiation and collagen-containing extracellular matrix without associated increases in chromatin accessibility, while corin also significantly reduces MPNST cell invasion. These data identify a specific influence of the LHC complex in regulating MPNST growth, cell death, differentiation and invasion and suggest that LHC inhibitors may prove useful in the treatment of this refractory malignancy.

Results

The LHC inhibitor, corin, blocks tumor cell growth and promotes apoptosis in MPNST

As previous studies have shown that inhibition of HDAC1, a component of the LHC complex, inhibits growth of MPNST cell lines harboring PRC2 complex mutations[10], we sought to determine the effect of our bi-functional HDAC1-LSD1 inhibitor, corin, on MPNST proliferation using a panel of ten established MPNST cell lines. Eight of the cell lines evaluated possessed inactivating mutations of NF1 and the PRC2 complex, while the remaining two cell lines originating from sporadic MPNSTs possessed wildtype NF1 and PRC2 (Table 1). All MPNST cell lines were treated with either DMSO, HDACi (entinostat), LSD1 inhibitor (GSK-LSD1) or corin and evaluated in a dose–response curve (Fig. 1A). Corin and entinostat treatment led to decreased proliferation across all cell lines tested without any notable response to GSK-LSD1 in any of the cell lines evaluated, consistent with data generated in other cell lines, where GSK-LSD1 does not affect cell proliferation[21,25]. Of note, the IC50 values for corin were consistently lower (1.4x-3.9x) than those observed for the HDACi, entinostat, across all cell lines (Table 1) with an IC50 range of 0.2–1.9 μM for corin versus 0.5–4.5 μM for entinostat. Additionally, all MPNST cells wildtype for PRC2 complex were less responsive to corin and HDACi (Fig. 1A, Table 1), consistent with previously published data[10]. Annexin V staining was performed to assess the impact of corin treatment on cellular apoptosis in two NF1/PRC2 wildtype MPNST cell lines (MPNST 724/STS26T) and two NF1-/PRC2- cell lines (S462/T265) using flow cytometry. Consistent with the dose–response data (Fig. 1A), corin induced apoptosis in all four cell lines tested (Fig. 1B, Supplementary Fig. 1) resulting in increased cell death in all cell lines treated with 1 μM corin (Fig. 1C). Notably, MPNST cells treated with DMSO, corin, or HDACi demonstrated significant cell death when visualized by phase contrast microscopy, with an elongated spindle-cell phenotype observed in T265 cells treated with corin (Fig. 1D).

Corin treatment of MPNST cells alters expression of axonogenesis and collagen-containing extracellular matrix genes independent of NF1 and PRC2 mutation status

Given the significant growth inhibitory and apoptosis-inducing effects of corin in MPNST cells, we next sought to determine the global transcriptional effects of LHC inhibition in PRC2 + /NF1 + and PRC2-/NF1- MPNST cells. S462, T265, MPNST724, and STS26T cells were treated with 1 μM corin for 24 h and evaluated by RNA-seq. Remarkably, hierarchical clustering of differentially expressed genes did not group cell transcriptional profiles based on NF1/PRC2 status (Fig. 2A). Principal Component Analysis (PCA) of differentially regulated genes further confirmed these findings, as MPNST cells treated with corin did not cluster according to NF1/PRC2 mutational status (Fig. 2B). When datasets from all four cell lines were combined and differential expression analysis was conducted, we identified 1,435 genes that were significantly upregulated by corin in the MPNST cell lines evaluated with an additional 103 genes that were significantly downregulated by corin (Fig. 2C). Further analysis of RNA-seq data from individual cell lines confirmed these results (Supplementary Fig. 2).Given that the LHC complex primarily functions by promoting repressive histone marks[26], it is not surprising that the vast majority of genes altered in expression following corin treatment were upregulated (Fig. 2A). We therefore chose to focus our subsequent data analyses on genes that were increased in expression following corin treatment. Examination of overlapping upregulated genes from all four MPNST cell lines identified 116 common genes with the greatest number of upregulated genes seen in T265 cells and the smallest number of upregulated genes

Cell line	Corin IC50 (μM)	HDACi IC50 (μM)	NF1 status	PRC2 status
MPNST 724	1.9 ± 0.8	4.5 ± 1.7	WT	WT
STS26T	1.3 ± 0.3	2.3 ± 0.3	WT	WT
S462	1.4 ± 0.5	3.5 ± 1.2	–	–
T265	0.4 ± 0.2	4.0 ± 3.4	–	–
ST8814	0.6 ± 0.04	0.9 ± 0.2	–	–
90-8	1.0 ± 0.4	0.8 ± 0.08	–	–
JH-2-031	0.7 ± 0.6	0.5 ± 0.2	–	–
JH-2-103	0.4 ± 0.05	0.8 ± 0.04	–	–
JH-2-079-c	0.2 ± 0.03	0.8 ± 0.07	–	–
JH-2-002	0.4 ± 0.1	0.7 ± 0.37	–	–

Table 1. Characteristics of MPNST cell lines used in this study and IC50 ± SEM (standard error of mean) where WT indicates wildtype gene (NF1, PRC2 complex) is present and – indicates an inactivating mutation is present in the associated gene of interest.

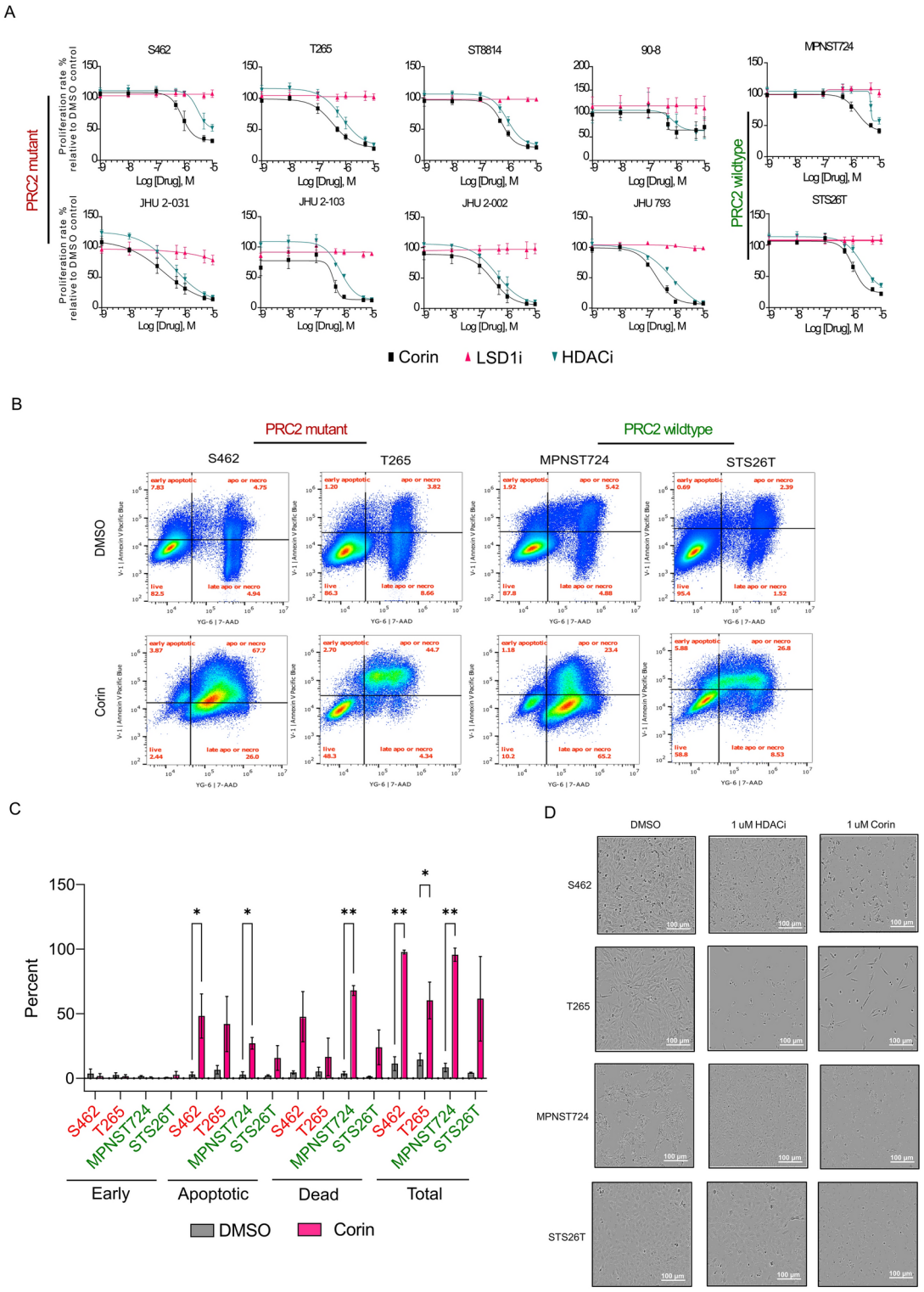

Fig. 1. The LHC inhibitor, corin, blocks tumor cell growth and promotes apoptosis in MPNST. (**A**) Dose–response curves for MPNST cells treated with DMSO, corin, HDACi (entinostat), or LSD inhibitor (GSK-LSD1). Treatment was for 72 h except for the four JHU cell lines which were treated for 120 h. Y axis represents proliferation rate normalized to DMSO. N = 4 (**B**) Flow cytometry analysis of MPNST cells treated with DMSO or 1 µM Corin for 72 h and stained with Annexin V. N = 3 (**C**) Quantification of apoptosis data in (**B**) for early apoptotic, apoptotic/necrotic and late apoptotic/necrotic cells treated with DMSO vs. corin. Cells in red font are PRC2 mutants and cells in green font are PRC2 wildtype. (**D**) Phase-contrast images of cells treated with DMSO or 1 µM Corin or HDACi for 72 h taken at 10X magnification. Paired t test was performed for apoptosis analysis of DMSO vs. corin treatment. *P < 0.05, **P < 0.01, ***P < 0.001.

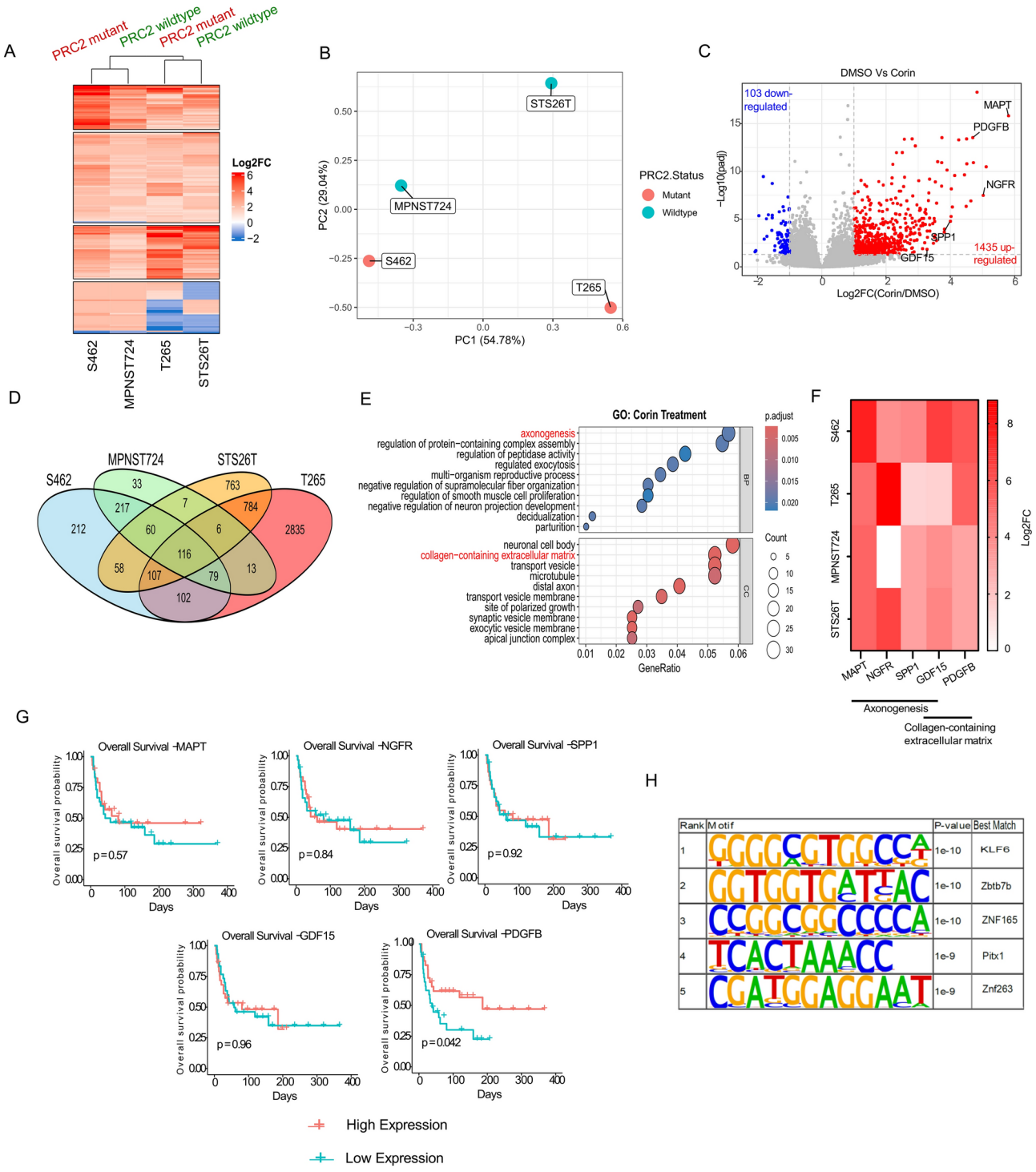

Fig. 2. Corin treatment of MPNST cells alters expression of axonogenesis and invasion genes independent of NF1 and PRC2 mutation status. (**A**) Heatmap and hierarchical clustering of genes differentially regulated by Corin in four MPNST cell lines. N = 2 (**B**) PCA plot for MPNST cells depicted in (**A**) following corin treatment. (**C**) Volcano plot representing differentially expressed genes (DEGs) in all four MPNST cell lines treated with corin. Red circles indicate genes upregulated by corin, while blue circles indicate gene downregulated by corin. Genes of interests are labeled. (**D**) Venn diagram illustrating the overlap of differentially upregulated genes among the four MPNST cell lines treated with corin. (**E**) Gene ontology analysis of the 1435 genes upregulated by corin in all four cell lines. BP: Biological process, and CC: Cellular component. (**F**) Heatmap of the five genes of interests labeled based on the GO analysis. (**G**) Kaplan Meier survival curves of the five genes. Kaplan Meier survival curves of the five genes (n = 59; "high" and "low" expression defined by median expression across patients). (**H**) Homer Motif analysis of the 1435 genes upregulated by Corin in all four cell lines.

seen in MPNST724 cells (Fig. 2D). The top gene ontology (GO) pathways for genes upregulated by corin revealed significant enrichment in biological processes including axonogenesis, as well as cellular components including neuronal cell body, collagen-containing extracellular matrix, distal axon, and synaptic vesicle membrane (Fig. 2E). These pathways suggest that the LHC complex influences MPNST differentiation and extracellular matrix dynamics. Consistent with this, GO analysis of differentially expressed genes in each cell line highlighted similar enriched pathways, including axonogenesis and collagen-containing extracellular matrix (Supplementary Fig. 3). The top five upregulated genes within these pathways—MAPT, NGFR, SPP1, GDF15, and PDGFB were subsequently analyzed and confirmed to be upregulated in the four MPNST cell lines, (Fig. 2F).

In order to determine the potential functional consequences of genes upregulated in MPNST cells following corin treatment, Kaplan–Meier survival curves were generated for the upregulated genes of interest using a MPNST patient cohort[27]. Among these genes, only PDGFB showed a significant positive association with survival outcome, where higher expression correlated with improved survival (Fig. 2G).

We next sought to identify transcription factors associated with increased gene expression following corin treatment of MPNSTs, and performed motif analysis of the 1435 differentially upregulated genes. The top hit in our analysis was KLF6, a known tumor-suppressor transcription factor regulating cellular senescence (Fig. 2H)[28,29]. Further analysis of transcription factor motifs associated with increased gene expression following corin treatment in each cell line identified enriched motifs associated with neuronal transcription factors including TFAP2A[30], RBPJ[31]and tumor suppressors including KLF4[32] and Osr1[33] (Supplementary Fig. 4).

Inhibition of the LHC complex promotes histone acetylation without a corresponding increase in chromatin accessibility

The catalytic activity of the LHC complex is mediated by both LSD1 and HDAC1. We have previously shown that the LHC complex modulates Histone 3 Lysine 9 acetylation (H3K9ac) and Histone 3 Lysine 27 acetylation (H3K27ac) in melanoma cell lines[21] and therefore sought to determine whether corin treatment of MPNST cells would alter H3K9/H3K27 acetylation and chromatin accessibility. We decided to only focus on these marks as histone methylation has been shown to not be highly affected by corin[21], and histone demethylation is not critical for the function of the CoREST complex in the epigenetic regulation of crucial tumor genes in some cancer types[20]. Four MPNST cell lines were treated with 1 μM Corin for 24 h and H3K9ac and H3K27ac levels were evaluated by western blot. Interestingly, a major increase in H3K27ac was only seen in S462 cells, while other cell lines showed an increase in H3K9ac (Fig. 3A,B) with the greatest increases noted in S462 cells. In order to evaluate chromatin accessibility changes associated with corin treatment of MPNST, S462 cells treated with DMSO, 1 μM corin, or 1 μM entinostat for 24 h were evaluated by ATAC-seq. Surprisingly, both corin and HDACi treatments led to a small decrease in chromatin accessibility in S462 cells. Heat map analysis of the ATAC-seq peaks reveals minimal differences in accessibility, suggesting that the observed decrease in accessibility is likely due to few loci, rather than a global reduction in accessibility (Fig. 3C). Annotation of the accessibility peaks across the genome revealed no notable differences between cells treated with DMSO, corin or the HDACi, entinostat, indicating that the decrease in accessibility does not occur at any of the genomic annotations measured (Fig. 3D). Additionally, visualizing individual gene tracks for the five genes identified in our RNA-seq experiments (Fig. 2F) revealed no significant differences in chromatin accessibility. However, we observe a non-significant decrease in chromatin accessibility in the promoter regions of MAPT and NGFR in response to corin treatment. Additionally, we observe a notable increase in chromatin accessibility in the promoter regions of SPP1 and GDF15 in response to Corin treatment (Fig. 3E).

Inhibition of the LHC complex leads to decreased tumor cell invasion in MPNST

RNA-seq data identified GO pathways associated with axonal differentiation and extracellular matrix pathways as being significantly enriched in corin-treated MPNST cells (Fig. 2). As these pathways are known to influence tumor cell metastatic phenotypes, we therefore investigated whether corin treatment of MPNST cells could impact tumor cell invasion. Five genes associated with neuronal differentiation or extracellular matrix composition which were identified as being significantly upregulated by corin in our RNA-seq studies were validated using qPCR (Fig. 4A) with all four cell lines demonstrating increased expression of the genes of interest following corin treatment. Boyden Chamber invasion assays were subsequently performed on all four MPNST cell lines to assess changes in MPNST invasion following 24 h treatment with 1 μM corin (Fig. 4B, 4C). All MPNST cell lines demonstrated reduced invasion following corin treatment with the most highly invasive cells lines in the DMSO controls (S462, STS26T) demonstrating the most significant decreases in invasiveness in response to corin. Overall, these findings suggest a critical role for the LHC repressor complex in mediating important tumorigenic functions in MPNST cells with LHC inhibition leading to decreased cell proliferation, increased apoptosis, increased cellular differentiation and decreased tumor cell invasion regardless of PRC2 status (Fig. 4D).

Discussion

In this study, we explore the role of the CoREST epigenetic repressor complex in regulating tumorigenesis in MPNST. Using the bifunctional small molecular inhibitor of LHC, corin, we demonstrate that the catalytic subunits of the CoREST complex are critical mediators of tumor cell proliferation, apoptosis and invasion of MPNST cells. Inhibition of the LHC complex by corin leads to a significant reduction in cell proliferation, with significantly greater effects than the HDACi, entinostat in all MPNST cell lines evaluated; however, NF1 + / PRC2 + tumor cells demonstrate decreased sensitivity to corin versus NF1-/PCR2- tumor cells (Fig. 1A and Table 1). Additionally, we find that corin induces apoptosis in MPNST cell lines regardless of their PRC2 mutational status (Fig. 1B); this is in contrast to the relative resistance of PRC2 + MPNST cells to apoptosis in the setting of

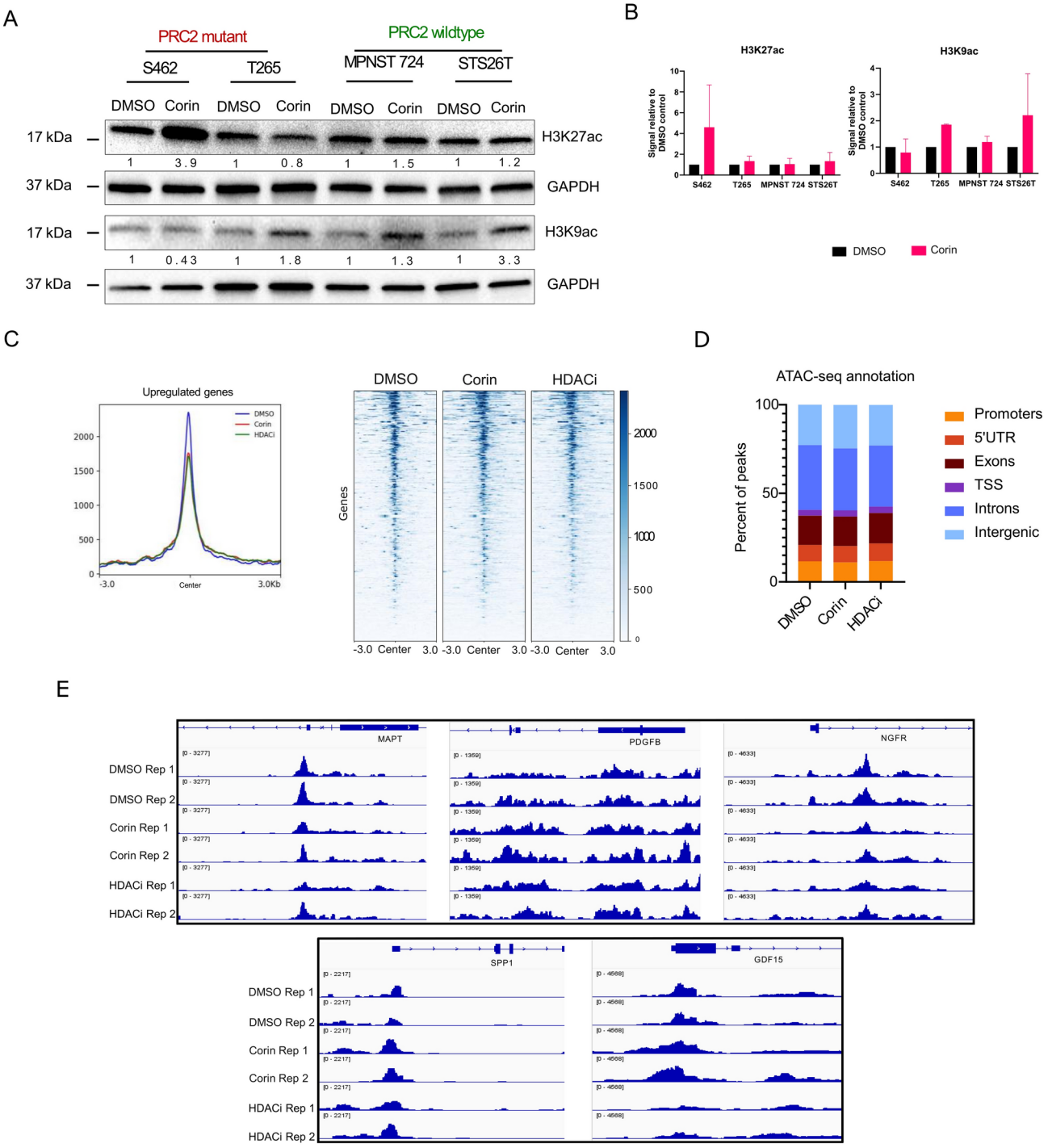

Fig. 3. Inhibition of the LHC complex promotes histone acetylation without a corresponding increase in chromatin accessibility. (A) Western blot of histone marks in PRC2 + (wildtype) and PRC2- (mutant) MPNST cells treated with DMSO vs corin. N = 2 (**B**) Bar graph quantifying the western blot in (**A**). (**C**) Plot profile and heatmap of chromatin accessibility in S462 MPNST cells treat with DMSO, corin or HDACi (entinostat). X axis represents the center of peak spanning -3 k to 3 k bp. Y axis represents the accessibility signal. (**D**) Genome annotation illustrating alteration of accessibility peaks at different genome annotations in S462 cells following treatment with DMSO, corin, or HDACi (entinostat). (**E**) Individual chromatin accessibility gene tracks for MAPT, PDGFB, NGFR, SPP1 and GDF15 in S462 cells following treatment with DMSO, corin or HDACi (entinostat) N = 2.

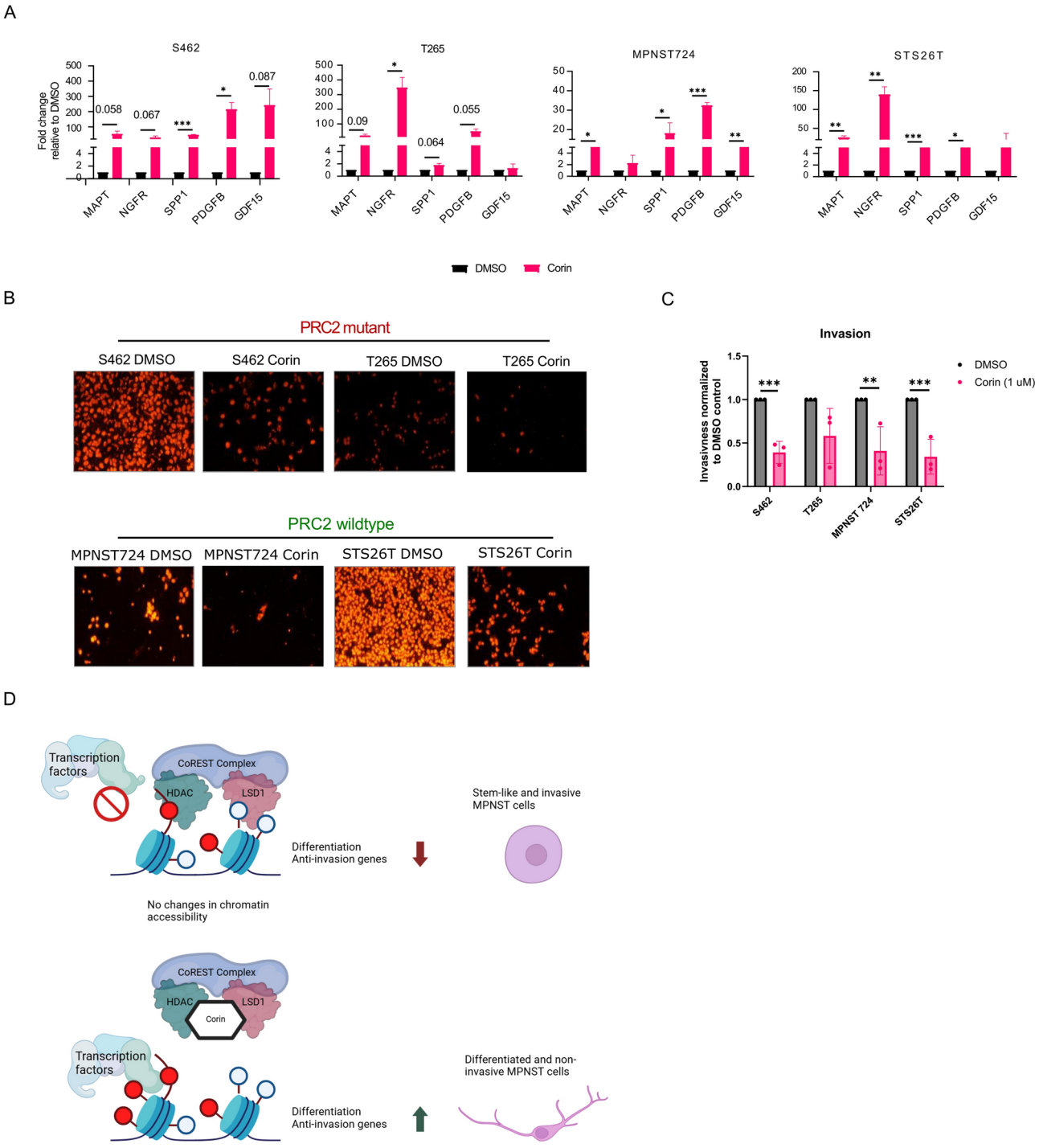

Fig. 4. Inhibition of the LHC complex leads to decreased tumor cell invasion in MPNST. (**A**) qPCR analysis of expression of genes of interest in S462, T265, MPNST724 and STS26T MPNST cells following treatment with DMSO or 1 μM corin for 24 h. N = 3 (**B**) Boyden chamber invasion assay of S462, T265, MPNST724 and STS26T MPNST cells treated with DMSO or 1 μM corin. N = 3 (**C**) Quantification of Boyden chamber invasion assay in S462, T265, MPNST724 and STS26T MPNST cells treated with DMSO or 1 μM corin. (**D**) Working model depicting the repressive function of the CoREST complex on the expression of differentiation and anti-invasion genes in MPNST cells by blocking the recruitment of differentiation and anti-invasion-associated transcription factors, leading to a a stem-like cell phenotype that is invasive. In MPNST, particularly in PRC2-null tumors, chromatin is in a highly open state. Treatment with corin inhibits the binding of the CoREST complex to chromatin leading to recruitment of differentiation and anti-invasion-associated transcription factors and the de-repression of differentiation and anti-invasion genes, resulting in a more differentiated and less invasive cell phenotype.

treatment with entinostat and other HDACi therapies[10,34]. Interestingly, previous studies have shown that the HDAC8-specific inhibitors PCI3 and PCI4 inhibit MPNST cell growth irrespective of PRC2 mutation status [35]; however, the IC50 for these reagents is 5–tenfold that of corin for a 96-h treatment regimen suggesting lower sensitivity to these reagents.

Transcriptomic analysis of corin-treated MPNST cells revealed significant upregulation of gene expression in all cell lines, with relatively few genes downregulated in response to corin (Fig. 2A, 2C) which is consistent with the LHC complex functioning as a transcriptional repressor complex and previous data in other cell lines[18–21,25]. Remarkably, we found top gene signatures upregulated in all MPNST cells treated with corin to include biological processes and cellular components associated with neuronal differentiation and axonogenesis which is consistent with CoREST complex functions as inhibitors of neuronal differentiation[36]. Some of the most significant genes identified as being upregulated in our RNA-seq experiments were MAPT, NGFR, SPP1, GDF15, and PDGFB. MAPT is a microtubule-associated protein with tumor-suppressive properties, with knockdown in clear cell renal cell carcinoma leading to increased tumor cell growth and invasion[37]. NGFR is a growth factor whose expression correlates with the activation of pro-apoptotic pathways[38]. SPP1 (secreted phosphoprotein-1) encodes the gene for osteopontin, an extracellular glycol phosphoprotein associated with diverse cellular functions due to a variety of distinct functional domains, proteolytically-cleaved and alternatively spliced variants, and numerous post-translational modifications[39]. Although originally identified as a highly phosphorylated protein present in bone matrix, subsequent studies have determined a wide-range of expression of SPP1 in mesenchymal cells and epithelial cells, with the highest levels of expression seen in brain tissue with associated neuroprotective functions including Schwann cell-derived peripheral axon regeneration[39,40]. GDF15, a member of the TGF-B superfamily, has been shown to reduce tumor cell proliferation and invasiveness and suppress epithelial-mesenchymal transition in cancer cells[41]. In addition, collagen-containing extracellular matrix pathways were among the top enriched GO signatures in all MPSNT cells treated with corin (Fig. 2E, Supplementary Fig. 2). One of the most upregulated genes in the collagen-containing extracellular matrix pathway was PDGFB (Fig. 2C, 2F), a member of the platelet-derived growth factor family which is typically seen as a homodimer (PDGF-BB) with known functions in angiogenesis[42], and Kaplan–Meier survival data indicated a significant survival advantage associated with higher PDGFB expression in MPNST. This was particularly surprising, given the known functions of PDGFB as a growth factor for mesenchymal cells which is primarily thought of as a tumor promoting growth factor in various cancers including lung, breast, and prostate cancer[43–45]; however, other studies suggest that functions of PDGFB may be tumor inhibitory and suppress metastasis due to specific effects on vascular remodeling and the extracellular matrix and depend on expression levels in vivo[42,46,47]. Thus, within the context of extracellular matrix remodeling, PDGFB may be an important mediator of the antitumor effects of corin in MPNST[47] which could account for corin-associated inhibition of tumor cell invasion (Fig. 4B, 4C). Consistent with the Gene Ontology (GO) data, transcription factor motifs associated with promoter regions of upregulated genes following corin treatment included binding sites associated with neuronal differentiation and tumor suppression.

ATAC-seq analysis of S462 cells demonstrated that genome-wide chromatin accessibility was slightly reduced in these PRC2-mutant MPNST cells following treatment with corin or the HDACi, MS-275 (Fig. 3C), despite increases in H3K27 acetylation and no changes in H3K9 acetylation (Fig. 3A, 3B) suggesting a more open chromatin structure[48]. Notably, basal chromatin accessibility, indicated by the large number of peaks identified in DMSO treated cells, was found to be high both genome-wide and at specific gene sites (Fig. 3C and 3E) in these PRC2-negative cells, which is not surprising given the repressor functions of the PRC2 complex[49] which are lost in these cells. These data therefore suggest that the primary function of corin in these tumor cells may involve altered transcription factor recruitment to chromatin rather than chromatin accessibility (Fig. 4D), which is consistent with a recent report suggesting that increases in chromatin accessibility within open chromatin regions does not necessarily correlate with gene expression changes[50].

Finally, we confirmed the upregulated expression of several genes associated with axonogenesis/neuronal differentiation and extracellular matrix remodeling in MPNST cells treated with corin and found that corin potently inhibits tumor cell invasion in MPNST cells irrespective of PRC2 status. Interestingly, recent studies using isogenic murine MPNST cell lines show that PRC2 loss in MPNST is a critical driver of tumor progression which leads to increased expression of matrix metalloproteinases (MMPs) and other matrix remodeling enzymes as well as increased collagen-dependent invasion and metastasis[51]. Thus, the anti-invasive properties associated with corin treatment of MPNST cells may be particularly worthwhile in PRC2-inactivated tumors.

MPNST is a highly aggressive tumor and the leading cause of death in patients with Neurofibromatosis Type 1. Despite significant advances in targeted and immunotherapy treatment of solid tumors over the past 3 decades, the prognosis for patients with MPNST has not changed substantially during this time and there are currently no FDA-approved systemic therapies for this aggressive malignancy (reviewed in[52]). Significant data suggests that epigenetic approaches to treat MPNST are warranted; however, no epigenetic therapies have proven successful in altering patient outcomes to date. Here, we show that the CoREST complex is a specific vulnerability in MPNST, particularly in PRC2-null tumors, and that the potent and specific bifunctional CoREST inhibitor, corin, demonstrates significant effects in inhibiting tumor cell growth, inducing apoptosis, promoting tumor cell differentiation and inhibiting tumor cell invasion in MPNST. Given the poor prognosis of this aggressive tumor with limited treatment options for advanced stages of disease, we suggest that further preclinical studies are warranted to explore the therapeutic potential of corin in patients with MPNST.

Materials and methods

Cell culture

The S462 and MPNST724 cell lines were graciously provided by Dr. Raphael Pollock. Additionally, the ST88-14, T265, 90–8, and STS26T cell lines were generously shared by Dr. Jeffrey Field. The JH-2–002, JH-2–031, JH-2-

079c, and JH-2–103 patient-derived MPNST cell lines [53] originated from the Johns Hopkins NF1 biospecimen repository[54,55] and were shared under Material Transfer Agreement from Johns Hopkins University. Other cell lines were cultured in high glucose DMEM with pyruvate (Thermo Fisher Scientific) supplemented with 10% Fetal Bovine Serum (FBS) and 1% penicillin/streptomycin. The JH patient derived cell lines were cultured in high glucose DMEM (Thermo Fisher Scientific) supplemented with 10% FBS and 1% penicillin/streptomycin. All cell lines were maintained at 37 °C and 5% CO2.

Compounds

The HDAC inhibitor Entinostat/MS275 (Cat. No.: HY-12163) and LSD1 inhibitor GSK-LSD1 (Cat. No.: HY-100546) were purchased from MedChemExpress. Corin was prepared as previously described[18]. All stock solutions were dissolved in DMSO.

Quanti-iT PicoGreen dsDNA cell proliferation assay

Cells were seeded in a 96-well and treated with the respective compound 24 h later. PicoGreen assay was done according to the manufacturer's suggested protocol (Thermo Fisher Scientific).

Apoptosis assay

Apoptosis was measured using the Pacific Blue™ Annexin V/SYTOX™ AADvanced™ Apoptosis Kit (ThermoFisher, A35136). The experimental protocol was performed according to the manufacturer's recommendations. Spectral flow analysis was performed using Cytek Aurora (Cytek Biosciences) according to the manufacturer's recommendations. Flow cytometry data was analyzed using SpectroFlo (v2.2) provided by Cytek Biosciences and FlowJo software (v10.10).

RNA extraction

S462, T265, MPNST724, and STS26T cells were treated for 24 h with 1 μM Corin or DMSO control treatment. RNA was extracted using the RNeasy Plus Mini Kit (Qiagen).

RNA-seq

Library was prepared and sequenced by Azenta Life Sciences. Reads were trimmed and low-quality reads were removed using Trimmomatic v.0.36. Reads were mapped to the GRCh38 reference genome using STAR aligner v.2.5.2b. Unique gene hit counts were calculated by using featureCounts from the Subread package v.1.5.2. Counts were used for differential analysis using DESeq2. The Wald test was used to generate p-values and log2 fold changes. Genes with an adjusted p-value < 0.05 and absolute log2 fold change > 1 were called as differentially expressed genes for each comparison. Heatmap and hierarchical clustering for the RNA-seq was generated using ComplexHeatmap v.2.20.0 [56]. PCA analysis was done using ggfortify v.4.4.1. Volcano plots were generated using ggplot2 and labeling was done using ggrepel. GO Plots were generated using the enrichGO and dotplot commands in clusterProfiler v4.12.0 [57]. Motif analysis was done using Samtools v.1.12 and homer v.4.1 using the findmotif.pl command searching for motifs within -400 to 100 bp of TSS.

Kaplan Meier survival curves

Kaplan Meier plots were generated using patient outcome and expression data [27]. Patients were excluded if mRNA expression analysis was unavailable, the patient died from other causes, or lacked follow-up. Plots and statistical analysis were performed in R using survfit from the survival package (v2.11–4).

Whole cell extracts and SDS-PAGE

Proteins were extracted from cells using M-PER lysis buffer according to the manufacturer's recommendations (Thermo Fisher Scientific). Protein concentrations were determined using the Pierce™ BCA Protein Assay (Thermo Fisher Scientific). 10 ug of whole cell extracts were separated on gradient 4–20% polyacrylamide precast gels (Bio-Rad) and transferred to PVDF membranes (Bio-Rad). Membranes were incubated with the following antibodies overnight: H3K9ac (ab32129), H3K27ac (ab4729), or GAPDH (sc-365062).

ATAC-seq

100,000 cells were seeded and treated with 1 μM Corin or DMSO. DNA was extracted, tagmented, purified, and adapter ligated using the ATAC-seq Kit (53,150) according to the manufacturer's instructions (Active Motif). Sequencing was done by Azenta Life Sciences and reads were trimmed using the fastp command in fastp v.0.23.4. Reads were aligned with GRCh38 reference genome using bowtie2 v.2.4.2. Sam files were filtered to retain the mapped reads only and converted to BAM files using Samtools v.1.12. Bed and Bedgraph files were created using Bedtools v.2.31.0. Peaks were called using Macs2 v.2.2.7.1 with the nomodel, and nolambda options. Bam files were normalized using RPKM to create BigWig files using the bamCoverage command in deeptools v.3.5.1. Deeptools was also used to create the matrix using the command computeMatrix, profile was created using the command plotProfile, and heatmaps were created using the command plotHeatmap. BigWig files were used to visualize individual gene tracks using IGV v.2.17.4. Genome annotation was done using Samtools v.1.12 and homer v.4.1 with the command annotatePeaks.pl.

cDNA preparation and qPCR

1 μg of RNA was reverse transcribed using the SuperScript III First-Strand Synthesis System kit (Invitrogen, Thermo Fisher Scientific). 40 cycles of qPCR were performed using the Step One Plus Real-time PCR System (Applied Biosystems). Data represents 3 biological replicates with 3 technical replicates per experiment. Primers used are listed in Supplementary Table 1.

Boyden chamber invasion assay

Transwell inserts (8 µm pore membrane) were placed in each well of a 24-well plate. 50 µg of Matrigel (Corning) diluted in 30 µL serum-free DMEM was added to each insert and incubated at 37 °C for 30 min. 150,000 cells were seeded in 300 µL serum-free DMEM media on the Matrigel in the top chamber and treated with 1 µM Corin or DMSO. 600 µL of 20% FBS DMEM was used as the attractant in the bottom chamber. After 24 h, cells and the Matrigel in the top chamber were removed, the membrane was washed with Phosphate-buffered saline (PBS), and fixed in 70% ethanol. The bottom of the membrane (where invading cells are located) was stained using 50 µg/mL propidium iodide and washed in PBS before cutting out the membrane. Stained membrane was visualized using the Nikon Eclipse E400 microscope and SPOT Advanced software. Five images at 20X were captured for each membrane. Image analysis was done using Fiji ImageJ using the method previously described[58]. A total of three biological replicates were done with three technical replicates done for each experiment.

Data availability

All the sequencing data generated are deposited in the GEO database (super series accession number: GSE275049, RNA-seq: GSE275048, ATAC-seq: GSE275047). Any additional information requested can be directed to the corresponding author. No codes were generated in the manuscript.

Received: 26 November 2024; Accepted: 14 March 2025
Published online: 24 March 2025

References

1. Yao, C. et al. Malignant peripheral nerve sheath tumors: Latest concepts in disease pathogenesis and clinical management. *Cancers* **15**, 1077 (2023).
2. Acem, I. et al. The association of metastasis pattern and management of metastatic disease with oncological outcomes in patients with malignant peripheral nerve sheath tumors: A multicenter cohort study. *Cancers* **13**, 5115 (2021).
3. Knight, S. W. E., Knight, T. E., Santiago, T., Murphy, A. J. & Abdelhafeez, A. H. Malignant peripheral nerve sheath tumors—A comprehensive review of pathophysiology, diagnosis, and multidisciplinary management. *Children* **9**, 38 (2022).
4. Cashen, D. V. et al. Survival data for patients with malignant schwannoma. *Clin. Orthop. Relat. Res.* **426**, 69 (2004).
5. Grobmyer, S. R., Reith, J. D., Shahlaee, A., Bush, C. H. & Hochwald, S. N. Malignant peripheral nerve sheath tumor: Molecular pathogenesis and current management considerations. *J. Surg. Oncol.* **97**, 340–349 (2008).
6. Gupta, G. & Maniker, A. Malignant peripheral nerve sheath tumors. *Neurosurg. Focus* **22**, 1–8 (2007).
7. De Raedt, T. et al. PRC2 loss amplifies Ras-driven transcription and confers sensitivity to BRD4-based therapies. *Nature* **514**, 247–251 (2014).
8. Zhang, X., Murray, B., Mo, G. & Shern, J. F. The role of polycomb repressive complex in malignant peripheral nerve sheath tumor. *Genes* **11**, 287 (2020).
9. Patel, A. J. et al. BET bromodomain inhibition triggers apoptosis of NF1-associated malignant peripheral nerve sheath tumors through bim induction. *Cell Rep.* **6**, 81–92 (2014).
10. Lopez, G. et al. Autophagic survival in resistance to histone deacetylase inhibitors: Novel strategies to treat malignant peripheral nerve sheath tumors. *Cancer Res.* **71**, 185–196 (2011).
11. Wojcik, J. B. et al. Epigenomic reordering induced by polycomb loss drives oncogenesis but leads to therapeutic vulnerabilities in malignant peripheral nerve sheath tumors. *Cancer Res.* **79**, 3205–3219 (2019).
12. Manta, A., Kazanas, S., Karamaroudis, S., Gogas, H. & Ziogas, D. C. Histone deacetylase inhibitors as a novel therapeutic approach for pheochromocytomas and paragangliomas. *Oncol. Res.* **30**, 211–219 (2022).
13. Trojer, P. Targeting BET bromodomains in cancer. *Annu. Rev. Cancer Biol.* **6**, 313–336 (2022).
14. Filippakopoulos, P. & Knapp, S. Targeting bromodomains: Epigenetic readers of lysine acetylation. *Nat. Rev. Drug Discov.* **13**, 337–356 (2014).
15. Kurimchak, A. M. et al. Resistance to BET bromodomain inhibitors is mediated by kinome reprogramming in ovarian cancer. *Cell Rep.* **16**, 1273–1286 (2016).
16. Mrakovcic, M. & Fröhlich, L. F. Molecular determinants of cancer therapy resistance to HDAC inhibitor-induced autophagy. *Cancers* **12**, 109 (2019).
17. Cooper, J. & Giancotti, F. G. Integrin signaling in cancer: Mechanotransduction, stemness, epithelial plasticity, and therapeutic resistance. *Cancer Cell* **35**, 347–367 (2019).
18. Kalin, J. H. et al. Targeting the CoREST complex with dual histone deacetylase and demethylase inhibitors. *Nat. Commun.* **9**, 53 (2018).
19. Anastas, J. N. et al. Re-programing chromatin with a bifunctional LSD1/HDAC inhibitor induces therapeutic differentiation in DIPG. *Cancer Cell* **36**, 528-544.e10 (2019).
20. Garcia-Martinez, L. et al. Endocrine resistance and breast cancer plasticity are controlled by CoREST. *Nat. Struct. Mol. Biol.* **29**, 1122–1135 (2022).
21. Wu, M. et al. The CoREST repressor complex mediates phenotype switching and therapy resistance in melanoma. *J. Clin. Invest.* **134**, e171063 (2024).
22. Kiuru, M. & Busam, K. J. The *NF1* gene in tumor syndromes and melanoma. *Lab. Invest.* **97**, 146–157 (2017).
23. Kochat, V. et al. Enhancer reprogramming in PRC2-deficient malignant peripheral nerve sheath tumors induces a targetable de-differentiated state. *Acta Neuropathol. (Berl.)* **142**, 565–590 (2021).
24. Karras, P. et al. A cellular hierarchy in melanoma uncouples growth and metastasis. *Nature* **610**, 190–198 (2022).
25. Almier, N. et al. Targeting the epigenome reduces keloid fibroblast cell proliferation, migration and invasion. *J. Invest. Dermatol.* https://doi.org/10.1016/j.jid.2024.06.1274 (2024).
26. Andrés, M. E. et al. CoREST: A functional corepressor required for regulation of neural-specific gene expression. *Proc. Natl. Acad. Sci. U. S. A.* **96**, 9873–9878 (1999).
27. Høland, M. et al. Transcriptomic subtyping of malignant peripheral nerve sheath tumours highlights immune signatures, genomic profiles, patient survival and therapeutic targets. *eBioMedicine* **97**, 104829 (2023).
28. Narla, G. et al. KLF6, a candidate tumor suppressor gene mutated in prostate cancer. *Science* **294**, 2563–2566 (2001).
29. Sabatino, M. E. et al. Krüppel-like factor 6 is required for oxidative and oncogene-induced cellular senescence. *Front. Cell Dev. Biol.* **7**, 297 (2019).
30. Hovland, A. S. et al. Pluripotency factors are repurposed to shape the epigenomic landscape of neural crest cells. *Dev. Cell* **57**, 2257-2272.e5 (2022).
31. Hu, Z.-L. et al. The role of the transcription factor Rbpj in the development of dorsal root ganglia. *Neural Develop.* **6**, 14 (2011).

32. Cercek, A., Wheler, J., Murray, P. E., Zhou, S. & Saltz, L. Phase 1 study of APTO-253 HCl, an inducer of KLF4, in patients with advanced or metastatic solid tumors. *Invest. New Drugs* **33**, 1086–1092 (2015).
33. Yu, Z. & Ouyang, L. OSR1 downregulation indicates an unfavorable prognosis and activates the NF-κB pathway in ovarian cancer. *Discov. Oncol.* **14**, 159 (2023).
34. Hirokawa, Y., Arnold, M., Nakajima, H., Zalcberg, J. & Maruta, H. Signal therapy of breast cancers by the HDAC inhibitor FK228 that blocks the activation of PAK1 and abrogates the tamoxifen-resistance. *Cancer Biol. Ther.* **4**, 956–960 (2005).
35. Lopez, G. et al. HDAC8, a potential therapeutic target for the treatment of malignant peripheral nerve sheath tumors (MPNST). *PLoS ONE* **10**, e0133302 (2015).
36. Sáez, J. E. et al. Decreased expression of CoREST1 and CoREST2 together with LSD1 and HDAC1/2 during neuronal differentiation. *PLoS ONE* **10**, e0131760 (2015).
37. Han, X. et al. Microtubule-associated protein tau (MAPT) is a promising independent prognostic marker and tumor suppressive protein in clear cell renal cell carcinoma. *Urol. Oncol. Semin. Orig. Investig.* **38**(605), e9-605.e17 (2020).
38. Chen, H. et al. NGFR increases the chemosensitivity of colorectal cancer cells by enhancing the apoptotic and autophagic effects of 5-fluorouracil via the activation of S100A9. *Front. Oncol.* https://doi.org/10.3389/fonc.2021.652081 (2021).
39. Yim, A., Smith, C. & Brown, A. M. Osteopontin/secreted phosphoprotein-1 harnesses glial-, immune-, and neuronal cell ligand-receptor interactions to sense and regulate acute and chronic neuroinflammation. *Immunol. Rev.* **311**, 224–233 (2022).
40. Wright, M. C. et al. Novel roles for osteopontin and clusterin in peripheral motor and sensory axon regeneration. *J. Neurosci. Off. J. Soc. Neurosci.* **34**, 1689–1700 (2014).
41. Tsui, K.-H. et al. Growth differentiation factor-15: A p53- and demethylation-upregulating gene represses cell proliferation, invasion and tumorigenesis in bladder carcinoma cells. *Sci. Rep.* **5**, 12870 (2015).
42. Hosaka, K. et al. Tumour PDGF-BB expression levels determine dual effects of anti-PDGF drugs on vascular remodelling and metastasis. *Nat. Commun.* **4**, 1–14 (2013).
43. Nordby, Y. et al. High expression of PDGFR-β in prostate cancer stroma is independently associated with clinical and biochemical prostate cancer recurrence. *Sci. Rep.* **7**, 43378 (2017).
44. Thies, K. A. et al. Stromal platelet-derived growth factor receptor-β signaling promotes breast cancer metastasis in the brain. *Cancer Res.* **81**, 606–618 (2021).
45. Xiu-Ying, H. et al. PDGFBB facilitates tumorigenesis and malignancy of lung adenocarcinoma associated with PI3K-AKT/MAPK signaling. *Sci. Rep.* **14**, 4191 (2024).
46. Prakash, J. & Shaked, Y. The interplay between extracellular matrix remodeling and cancer therapeutics. *Cancer Discov.* **14**, 1375–1388 (2024).
47. Zhang, Y. et al. Platelet-specific PDGFB ablation impairs tumor vessel integrity and promotes metastasis. *Cancer Res.* **80**, 3345–3358 (2020).
48. Klemm, S. L., Shipony, Z. & Greenleaf, W. J. Chromatin accessibility and the regulatory epigenome. *Nat. Rev. Genet.* **20**, 207–220 (2019).
49. Liu, X. & Liu, X. PRC2, chromatin regulation, and human disease: Insights from molecular structure and function. *Front. Oncol.* **12**, 894585 (2022).
50. Kiani, K., Sanford, E. M., Goyal, Y. & Raj, A. Changes in chromatin accessibility are not concordant with transcriptional changes for single-factor perturbations. *Mol. Syst. Biol.* **18**, e10979 (2022).
51. Brockman, Q. R. et al. PRC2 loss drives MPNST metastasis and matrix remodeling. *JCI Insight* **7**, e157502 (2022).
52. Somatilaka, B. N., Sadek, A., McKay, R. M. & Le, L. Q. Malignant peripheral nerve sheath tumor: Models, biology, and translation. *Oncogene* **41**, 2405–2421 (2022).
53. Wang, J. et al. Combined inhibition of SHP2 and MEK is effective in models of NF1-deficient malignant peripheral nerve sheath tumors. *Cancer Res.* **80**, 5367–5379 (2020).
54. Banerjee, J. et al. Integrated genomic analysis of NF1-associated peripheral nerve sheath tumors: An updated biorepository dataset. *bioRxiv* https://doi.org/10.1101/2024.01.23.576977 (2024).
55. Pollard, K. et al. A clinically and genomically annotated nerve sheath tumor biospecimen repository. *Sci. Data* **7**, 184 (2020).
56. Gu, Z., Eils, R. & Schlesner, M. Complex heatmaps reveal patterns and correlations in multidimensional genomic data. *Bioinformatics* **32**, 2847–2849 (2016).
57. Wu, T. et al. clusterProfiler 4.0: A universal enrichment tool for interpreting omics data. *Innovation* **2**, 100141 (2021).
58. Schroeder, A. B. et al. The ImageJ ecosystem: Open-source software for image visualization, processing, and analysis. *Protein Sci. Publ. Protein Soc.* **30**, 234–249 (2021).

Acknowledgements

R.A. and M.C. are supported by a Department of Defense Translational Research Award in Melanoma (W81X-WH-21-1-0980); P.A.C. is supported by NIH grant R35 GM149229. We thank Dr. Anna Belkina for her expertise and assistance with FACS protocols and data analysis. We thank Dr. Raphael Pollock for providing S462 and MPNST724 cell lines. We thank Dr. Jefferey Field for providing ST88-14, T265, 90-8, and STS26T cell lines. We thank Dr. Christine Pratilas for providing JH-2-002, JH-2-031, JH-2-079c, and JH-2-103 cell lines.

Author contributions

Conceptualization: RMA; Experimental Design/Data Curation: IS, RF, SB, MC, RMA; Formal Analysis: IS, RF, MC, RMA; Supervision: MC, PAC, RMA; Writing – Original Draft: IS, RMA; Writing – Review and Editing: IS, RF, SB, MC, PAC, RMA.

Declarations

Competing interests

PAC is a co-founder of Acylin Therapeutics and a consultant for Abbvie regarding p300 acetyltransferase inhibitors. He also is a co-inventor on a US patent application for corin (US patent no. 11,565,994). RMA is a co-founder of Acylin Therapeutics. All other authors have no competing interest.

Additional information

Supplementary Information The online version contains supplementary material available at https://doi.org/10.1038/s41598-025-94517-w.

Correspondence and requests for materials should be addressed to R.M.A.